JSAE 20119156
SAE 2011-01- 1982

Investigation of Fuel Effects on Spray Atomization and Evaporation Studied for a Multi-hole DISI Injector with a Late Injection Timing

Lars Zigan[1, 2], Markus Ammon[1], Ingo Schmitz[1, 2], Michael Wensing[1, 2], Alfred Leipertz[1, 2]
[1]Lehrstuhl für Technische Thermodynamik, Universität Erlangen-Nürnberg
[2]Erlangen Graduate School in Advanced Optical Technologies (SAOT),Universität Erlangen-Nürnberg

Vivek Gupta
Indian Institute of Technology (IIT) Roorkee, Uttarakhand, India - 247667

ABSTRACT

The influence of fuel composition on sprays was studied in an injection chamber at DISI conditions with late injection timing. Fuels with high, mid and low volatility (n-hexane, n-heptane, n-decane) and a 3-component mixture with similar fuel properties like gasoline were investigated. The injection conditions were chosen to model suppressed or rapid evaporation. Mie scattering imaging and phase Doppler anemometry were used to investigate the liquid spray structure. A spray model was set up applying the CFD-Code OpenFOAM. The atomization was found to be different for n-decane that showed a smaller average droplet size due to viscosity dependence of injected mass. And for evaporating conditions, a stratification of the vapor components in the 3-component fuel spray was observed.

INTRODUCTION

Among the different combustion concepts of gasoline engines with direct injection, the spray-guided technologies with charge stratification offer the highest potential to reduce fuel consumption. In spray-guided direct injection spark ignition (SG-DISI) engine concepts, the central position of the injector with a small distance to the spark plug is preferred. Under partial load conditions, charge stratification is preferable to reduce fuel consumption. For operating points with late injection, the fuel is injected into a pressurized cylinder and, close to the spark plug an ignitable mixture is positioned. The main challenge is to ensure an ignitable mixture at the spark plug for all engine operating points when applying different worldwide available fuel compositions. A high amount of synthetic or regenerative fuel components like ethanol in gasoline mixtures can significantly change the mixture formation and combustion processes, especially in those SG-DISI-engine concepts. This fuel impact on spray behavior can be hardly predicted by current CFD-models (Computational Fluid Dynamics) as they are based on simplified correlations not covering fuel-dependent cavitation and atomization behavior. Additionally, models based on diesel injection may not properly work for gasoline injectors as well [1]. Regarding fuel-dependent spray atomization, only few fundamental studies using simple throttle or model nozzle geometries were published in the literature [2, 3] where the cavitation and turbulent flow behavior are very different from realistic multi-hole nozzles. Furthermore, most of the spray process steps and their interactions are still not well understood [4]. Therefore, measurement data of the spray process including the turbulent nozzle flow, atomization, evaporation and droplet collision effects are necessary for a deeper insight into spray processes and model improvements. Especially, the fuel dependent atomization and evaporation of single and multi-component fuels are still discussed in the literature.

Kelly-Zion et al. [5] measured the qualitative vapor distribution and mixing of a low and high volatility component in a port fuel injection SI engine using two laser-induced-exciplex fluorescence techniques (LIEF). It was observed that batch distillation takes place already in the suction duct. Therefore, the liquid entering the cylinder is mostly composed of the heavy boiling components of the fuel. Also for direct injection engines with early injection and near ambient gas temperatures, a distillation-like evaporation can be assumed i.e. the release of light and heavy ends takes place at different times and locations in the cylinder. High volatility fuel components evaporate faster and low volatility components remain in the droplet and determine the droplet evaporation and breakup at

later droplet lifetimes. However, the long mixing time and charge motion in the intake and compression stroke enhances mixing of the light and heavy boiling ends in the vapor phase with air, so that almost no vapor component stratification takes place for early injection. This behavior was described by Williams et al. [6] who applied three fuel tracers with different volatility in laser-induced fluorescence measurements.

Han and Steeper [7] conducted experiments with a two-component fuel doped with three fluorescent tracers of different volatility classes in an engine. For late injection timing, an incomplete mixing of the different fuel components at ignition time was found. Also a demixing of the fuel components was shown by Egermann and Leipertz [8] with Raman-measurements in an evaporating two-component fuel spray of high volatility benzene and the high boiling point fuel n-decane in a 1:1 mixture. The measurements were conducted in a high pressure-high temperature injection chamber at 3.0 MPa and 250°C.

In contrast to this, Hoffmann et al. [9] detected a very similar vapor distribution of different boiling point fuel components for sprays at diesel engine conditions (injection pressure p_F = 60 MPa, chamber pressure p_c = 5 MPa, chamber temperature ϑ_c = 527°C) by means of laser-induced fluorescence indicating a very rapid evaporation, i.e., a co-evaporation of the fuel components occurs. From this, it can be concluded that the multi-component fuel spray evaporation under a high pressure atmosphere is still a research topic with many open questions. Especially, there is still a lack of quantitative information about the fuel vapor distribution at the spark plug at the point of ignition for SG-DISI engines with late injection. A stratification of fuel components changes the local fuel/air ratio and controls the ignition, combustion and pollutant formation. The spark plug is usually positioned at 10-15 mm from the injector nozzle for spray-guided concepts and ignition starts approximately 1 to 2 ms after start of injection for stratified engine operating conditions in the presence of evaporating droplets.

For a deeper insight into atomization and evaporation processes, in this study a 3-component fuel was observed in comparison with several single component model fuels in an optical accessible pressurized and heated injection chamber. The liquid spray structures and evaporating droplets of a 12-hole solenoid DISI-injector were analysed by Mie imaging and phase Doppler anemometry (PDA). A simplified 3-component fuel was chosen to describe effects of main fractions in the fuel. This fuel mixture was proved and validated to model the realistic spray behavior of a multi component gasoline fuel under charge stratification conditions [10, 11]. Also, a numerical implementation of this simplified surrogate fuel into CFD (Computational Fluid Dynamics) reduces the computational effort. For this, the open source code OpenFoam 1.5 was applied.

EXPERIMENT AND MODEL DEFINITION

MODEL FUEL AND EXPERIMENT

A chamber pressure of 1.5 MPa and a temperature of 400°C were chosen to model late injection timing. These conditions refer to the end of injection close to the ignition time point, see Figure 1. For this injector, the investigated operating point refers to an indicated mean effective pressure (imep) of approximately 2.7 bar.

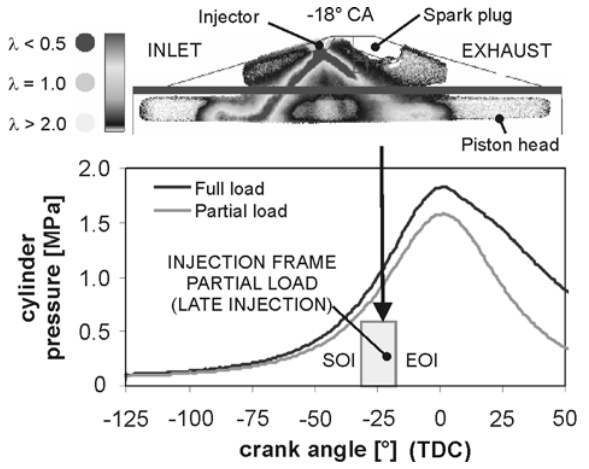

Figure 1: Optical accessible engine with arrangement of the injector close to the spark plug and typical injection frames for partial load conditions. Recording time point is 18°CA (crank angle) before TDC

Additionally, the experiments were also conducted at 20°C and 1.5 MPa to study the fuel dependent atomization. A constant air flow through the injection chamber heats the chamber and scavenges it from one injection to another (air flow velocity < 0.2 m/s) by an injection repetition rate of 1 Hz. The fuel and the injector were conditioned to 70°C similar to engine wall temperatures. The injection pressure was set to 10 MPa with a flexible fuel system. The controlling time of the solenoid- injector (BOSCH, based on the HDEV1.2 with a conical nozzle tip) was kept constant for all investigated fuels at 700 µs, however, an effective injection time of 950 µs results due to a delayed needle closure. A small injected mass of approximately 6.5 mg/pulse was adjusted in accordance to the partial load operating point.

The broad boiling range of gasoline fuels can be modeled with mixtures of n-alkanes (see Table 1).

Table 1: Fuel properties at atmospheric boundary conditions (25°C, 0.1 MPa) [12-15]

	hexane	heptane	decane	3-comp. f.	gasoline
ρ [kg/m^3]	656	664	717	705	720-775
ϑ_B [°C]	66	99	176	66-176	35-210
σ [mN/m]	17.89	19.65	23.37	19.78	22.00
ν [10^{-6} m^2/s]	0.45	0.58	1.21	0.57	0.53 [1]
p_v [kPa]	19.90	6.06	0.171	-	45.00

ρ = density, ϑ_B = normal boiling point, σ = surface tension, ν = kinematic viscosity, p_v = vapor pressure

During this study, a surrogate 3-component fuel was used to model the boiling curve of gasoline. It contains 35% (by volume) of n-hexane with high volatility, 20% of the high boiling point fuel n-decane, and 45% of n-heptane which covers the middle part of the gasoline boiling range.

To describe the macroscopic spray propagation of the liquid phase, an integral Mie scattering technique using illumination by flash lamps was applied, see Fig. 2. Integral Mie Imaging and phase Doppler anemometry were used consecutively.

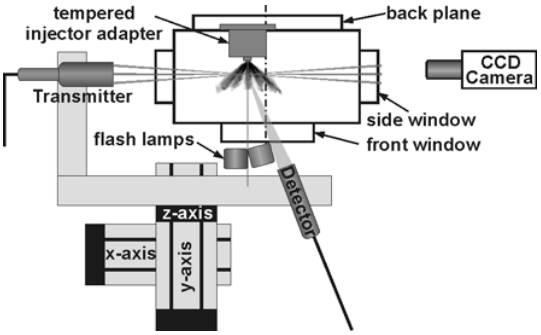

Figure 2: Experimental setup to study the fuel dependent liquid spray structure

The scattered light was detected perpendicular to the measurement plane with a CCD camera with 1,280x1,024 pixels and a dynamic range of 12 bit. Averaged images were calculated from 32 single-shot images. Droplet size and velocity measurements were performed using phase Doppler anemometry in a distance of 10, 15, and 20 mm from the injector tip in several measurement locations, see Fig. 3. The beams of a 5 W argon ion laser (514.5 and 488.0 nm) were split into two parts and utilized for the laser Doppler anemometer.

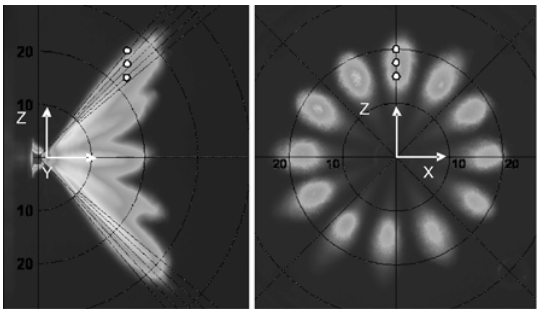

Figure 3: Integral (left) and radial light sheet illuminated sprays (right) with marked PDA-measurement locations in a plane 15 mm from injector tip; Images taken for n-decane at 1,250 µs after visible start of injection (v. SOI), non-evaporating conditions; (image taken from [16])

The laser beams, one of them shifted in frequency by 40 MHz, were overlapped in an intersection volume by a transmitter optic using a 310 mm collimator lens. The resulting probe volume contained 18 fringes with a fringe spacing of about 4 µm. The used fiber PDA analysis system leads to a droplet size measurement range of up to 140 µm. The probe volume was positioned within the spray field using a three-dimensional traversing unit. The scattered light was detected using an optical receiver with a lens of 300 mm focal length and a receiving aperture mask for small particles. The Brewster angle was chosen for signal detection in order to make the PDA arrangement most insensitive for changes in refraction index due to fractionation and temperature rise in the boiling droplets. For a statistical analysis, 1,200 injections at each measurement location were conducted and 20,000 validated bursts were defined as an abort criterion, respectively. Further details of the PDA measurement setup can be found in ref [16]. For calculation of the droplet size distributions, the droplet size intervals were kept constant for all fuels with an interval width of 0.81 µm ranging from 0.1 to 50 µm.

MODEL DEFINITION

Spray model

The spray propagation was simulated for a pressure chamber with a mesh volume of 20 x 20 x 50 mm^3 with the 3D-CFD-Code OpenFoam 1.5. Only one jet of the 12-hole injector was modelled since there were no jet-to-jet interactions in the experiments, see Fig. 3. For this, an Euler-Lagrange approach in the RANS context (Reynolds Averaged Navier Stokes) was applied. The inner region of the mesh had a finer resolution (0.32 x 0.32 x 1 mm) and contains the whole spray, see Fig. 4. The nozzle outlet was defined 0.5 mm inside the grid to avoid numerical errors. The surrounding atmosphere was defined as quiescent at initial conditions. The Rail pressure in the experiments was adjusted to be 10 MPa, however, the fuel pressure in the injector was defined to be lower (6.4 MPa) according to the pressure drop in the throttle, at the needle seat and the nozzle holes.

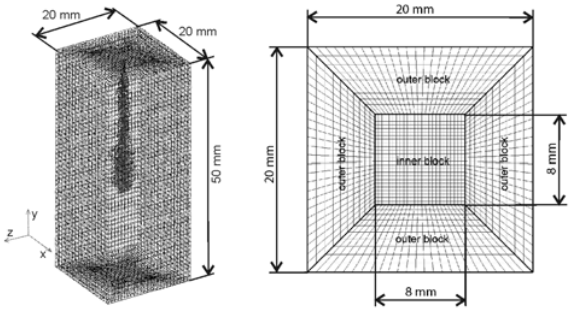

Figure 4: Mesh for spray calculation shown for a typical jet at 1.000 µs after SOI (left); a finer mesh was applied in the spray region (inner block) and a coarser one at the outer regions

The initial spray angle of the single jet was 20°, which was assumed as constant during the whole injection duration. The nozzle diameter was 125 µm, see Table 2. The initial droplet diameter range of 1-120 µm was generated by a Rosin-Rammler distribution which showed a peak at 60 µm, see Fig. 5. For a statistical representation of the liquid phase in the Lagrangian formulation of the discrete droplet model, a certain number of parcels were defined to represent different groups of identical drops. The number of parcels defines the accuracy of the spray model. It was

pointed out that 5,000 parcels were sufficient to model the spray in terms of spray shape, penetration and droplet size distribution.

Table 2: Injection model parameters

Injection parameter	value
Injection pressure p_F	6.4 MPa
Spray angle	20°
Nozzle bore diameter d_0	125 µm
Fuel temperature ϑ_F	70°C
Number of computational parcels	5,000

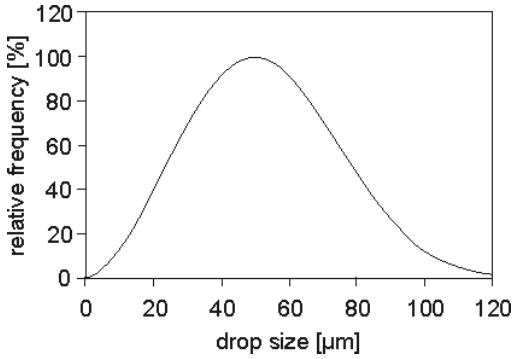

Figure 5: Initial drop size distribution at the nozzle exit modeled by a Rosin-Rammler function

The utilized sub-models for the spray processes atomization, collision, turbulent droplet dispersion, evaporation as well as droplet drag and turbulence are given in Table 3.

Table 3: Applied spray models of the calibrated CFD-Model

Sub-process	Model
Droplet drag	Standard
Turbulence	RNG-k-epsilon
Droplet breakup	ETAB
Collision	trajectory
Droplet dispersion	Stochastic dispersion
Evaporation	Infinite diffusion model

The droplet breakup due to aerodynamic forces has been accounted for by the ETAB-model (Enhanced Taylor-Analogy Breakup) proposed by Tanner [17]. This model is based on an approach by O'Rourke and Amsdan [18] that describes the droplet deformation as a one-dimensional, harmonic, damped oscillation in analogy to a spring-mass system. The included oscillation frequency ω and the deformation time t_d are defined as following:

$$\omega^2 = \frac{64\sigma}{\rho_d d^3} - \frac{1}{t_d^2} \quad (1)$$

$$t_d = \frac{\rho_d d^2}{10\eta_L} \quad (2)$$

The included parameters are the liquid dynamic viscosity η_L, the surface tension σ, the fuel density ρ_d and the droplet diameter d. The droplet breakup occurs for Weber numbers We > 6. In the Weber number, the density of the ambient gas ρ_g, the droplet radius r_d, the relative velocity between droplet and gas u_{rel} as well as the surface tension σ is included:

$$We = \frac{\rho_g r_d u_{rel}^2}{\sigma} \quad (3)$$

Two limiting cases were considered: one for low Weber number around six and other for stripping breakup for very large Weber numbers. In the first case breakup occurs when $\omega t_{bu} = \pi$. For high Weber numbers in the stripping breakup regime, the breakup happens much earlier in the oscillation period, i.e. when $\omega t_{bu} << \pi$. The breakup time t_{bu} for the respective regime are defined as:

$$t_{bu} = \begin{cases} \pi\sqrt{\frac{\rho_d d^3}{64\sigma}} & \text{(bag breakup)} \\ \sqrt{3}\,\frac{r_d}{u_{rel}}\sqrt{\frac{\rho_d}{\rho_g}} & \text{(stripping breakup)} \end{cases} \quad (4)$$

The resulting droplet size (radius r_d) was calculated according to Tanner [17]:

$$\frac{r_d}{r_{d,0}} = \exp\left[-K_{bu} t_{bu}\right] \quad (5)$$

$$K_{bu} = \begin{cases} k_1\omega & \text{(bag breakup)} \\ k_2\omega\sqrt{We} & \text{(stripping breakup)} \end{cases}$$

The equations contain a breakup parameter K_{bu} depending on the breakup regime and, therefore the Weber number. The two correction factors k_1 and k_2 are defined in the model with an default value of 0.2 and will be discussed later.

In the original collision model of O'Rourke [19], the droplet interactions are described statistically with probability density functions in which the parcels tend to collide if they are in the same cell. The collision frequency depends on the computational grid size irrespective of the droplet velocity vector or position in the cell. To compensate this, the trajectory-model proposed by Nordin [20] was applied, which is an advancement of O'Rourke's model formulation, in which the collision occurs if the trajectories of two parcels intersect at a certain collision time even if they are in different cells. However, in both models either droplet coalescence or bouncing is considered, but droplet breakup or separation is neglected.

To describe the droplet evaporation, the infinite diffusion model (or infinite conductivity) was used. For multi-component fuels, the species concentration (which is spatially uniform in distribution inside the droplet) and the droplet temperature depend only on time. This is valid for the liquid fuel having infinitely large heat conductivity which is enhanced by forced

convection. Due to a high relative velocity between the droplet and surrounding gas, a circulating flow inside the droplet is induced that supports the internal mixing. This approach is limited to a rapid heat and mass transfer [21], which is true for high ambient temperature and high velocities, e.g. for diesel injection in vicinity of the nozzle [22]. However, the original single-component fuel evaporation model was enhanced to represent the proposed 3-component fuel in which different fuels were treated independently in the same but well mixed droplet. With this, the spatial distribution of the major components of a commercially available gasoline fuel was indicated.

Single droplet model

Additionally, a single droplet model was used to describe the evaporation behavior of the different fuel components in a substitute droplet with average quantities of the spray. Therewith, the influences of atomization, collision and spray-induced turbulence can be separated. In the evaporation model, the heat conduction and convection between droplet and gas was considered, however, radiation and real gas effects were neglected. The investigated substitute droplet had a droplet size of 20 µm, an initial temperature of 70°C and was assumed to be quiescent as the droplet decelerated very fast. The computational domain was reduced to 150 cells and only one parcel with the mass of a single droplet was defined.

RESULTS AND DISCUSSION

MODEL CALIBRATION

The numerical spray model was calibrated with experimental data of the spray shape, spray penetration and the droplet size distributions. Especially, for the breakup model careful adjustment of the breakup parameters was necessary. The two breakup parameters k_1 and k_2 of the corresponding atomization regime were tuned keeping other model parameters constant. The calibration was conducted for n-decane at a chamber pressure of 1.5 MPa and ambient temperatures of 20 or 400°C, respectively. An increased value of k_1 accelerates the breakup of low Weber numbers and leads to smaller droplets. The parameter k_2 controls the droplet breakup at high Weber numbers in vicinity of the nozzle. The default value produces a rapid breakup with too small droplets and a slim spray. The most appropriate values of these parameters are k_1 = 0.15 and k_2 = 0.015 (non-evaporating case: 0.03) for the current injection conditions.

In general, a good agreement of the global shape between the calibrated spray and the experimental spray was achieved, see Fig. 6. To show the temporal behaviour of the spray propagation, in the left half of the image, the experimental results of the integral spray illumination were compared with the numerical experiments that are displayed at the right side. The single shot images were taken to represent the turbulent spray structure, which appears more blurred in the averaged images. A similar trend of the spray cone angle, the spray length and the broadened spray front can be predicted by the model.

The penetration of the experimental and numerical spray is shown in Fig. 7 (top), where a good agreement is visible. Also the droplet size distribution is well represented by the model; the arithmetically averaged droplet size d_{10} and the Sauter mean diameter d_{32} are precisely matched (Fig. 7, bottom).

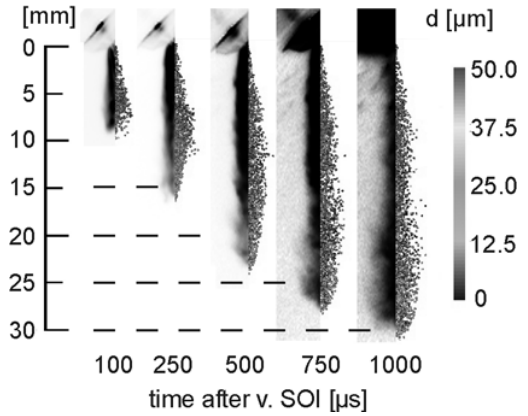

Figure 6: Experimental Mie-scattering images (left) and calibrated spray model (right) at evaporating conditions (ϑ_C = 400°C, p_C = 1.5 MPa), n-decane

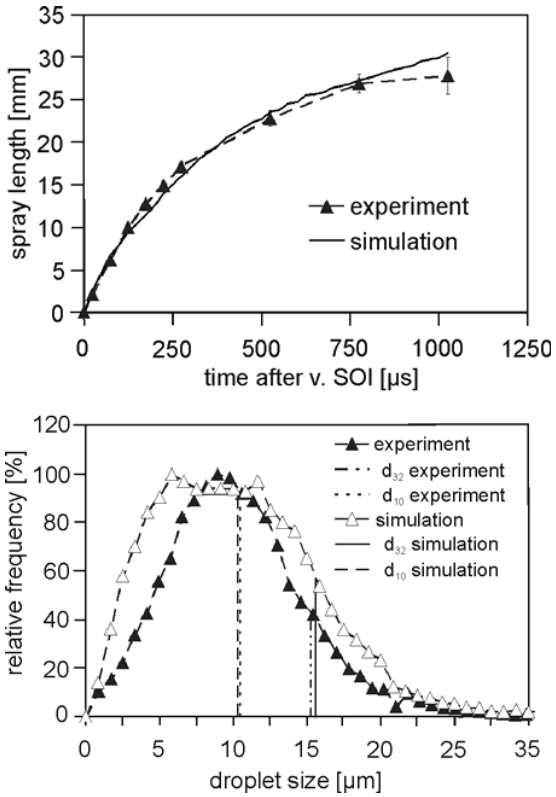

Figure 7: Comparison of the experimental and numerical spray penetrations (top) and drop size distribution (bottom), averaged over the whole injection time across the measurement points in the plane at 15 mm from the nozzle tip, n-decane, p_c = 1.5 MPa, ϑ_c = 400°C, ϑ_F = 70°C

However, for the model the larger droplets are more pronounced, which is due to the model assumptions.

In the experiment, less small droplets were detected due to the limitations of the measurement technique in dense sprays at high pressure. The validation of the spray model was conducted with the experimental data of atomization and evaporation rates of different fuels. Therewith, the vapor distribution of a 3-component fuel was verified.

SPRAY BEHAVIOR AT SUPRESSED EVAPORATION

Firstly, the fuel dependent atomization behaviour was studied at ambient pressure of 1.5 MPa and 20°C (these values are referred to as 'suppressed evaporation conditions'). To validate the atomization, the Ohnesorge (*Oh*), liquid Weber (We_L) and Reynolds (Re_L) numbers, which describe the regime of the primary spray breakup, were calculated:

$$\mathrm{Oh} = \frac{\eta_L}{\left(\rho_L \sigma d_0\right)^{0.5}} \tag{6}$$

$$\mathrm{We_L} = \frac{\rho_L d_0 u_L^2}{\sigma} \tag{7}$$

$$\mathrm{Re_L} = \frac{\rho_L d_0 u_L}{\eta_L} \tag{8}$$

The included properties are liquid density ρ_L, dynamic viscosity η_L, surface tension σ, velocity u_L and the nozzle bore diameter d_0. The Injection velocities were calculated from measured averaged mass flow which is approximately 75 m/s. Those non-dimensional numbers are very similar for n-hexane, n-heptane and the 3-component fuel, however, larger differences exist for n-decane, see Table 4.

Table 4: Ohnesorge, liquid Weber and Reynolds numbers for the tested fuels under measurement conditions

	n-hexane	n-heptane	n-decane	3-comp.f.
Oh	0.00650	0.00737	0.01237	0.00716
Re	30,357	24,779	12,552	25,215
We_L	38,992	34,611	30,042	34,754

A small Reynolds number indicates a lower turbulent intensity which reduces the droplet breakup. This is also reflected by a small Weber number that was determined by a high surface tension and fuel density and lead to a slow breakup process. However, this effect was more dominant under low temperature conditions as discussed below for the comparison of generated drop sizes between n-decane and n-heptane. Further aspects are considered in refs. [10, 24].

Fig. 8 shows the average images of the different fuel sprays at 1,000 µs after visible start of injection (v. SOI). Optical dense spray regions (with high droplet load) show high intensity of the scattered light. Under low chamber temperature conditions (20°C, left column), the spray shapes are very similar for all fuels. For n-decane, the signal intensity close to the nozzle is lower which displays a decreased droplet density and indicates that fuel properties change the spray breakup which will be discussed below. The influence of the fuel composition on spray shape is more considerable for high ambient temperatures (right column). After 1,000 µs, right after end of injection, almost no liquid fuel was detected for n-hexane and the penetration of the liquid spray front decreased. For n-decane, n-heptane and the 3-component fuel, still liquid fuel was detected at later times. Also, the thickness of each jet and the droplet load is dependent on the boiling characteristics of the fuels.

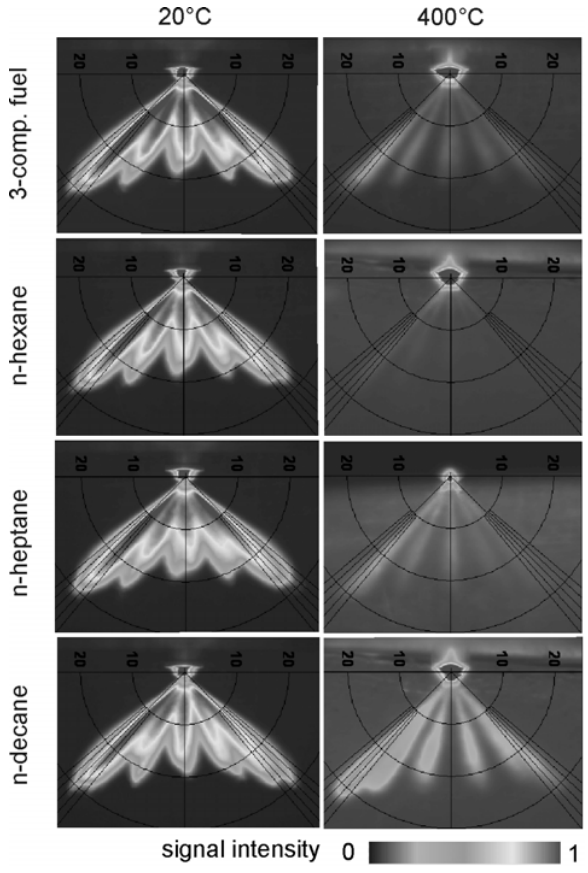

Figure 8: Fuel dependent spray propagation at 1,000 µs after v. SOI at high chamber pressure (1.5 MPa) and air temperatures of 20°C (left) and 400°C (right)

PDA measurements were conducted to describe the effect of the fuel properties on the droplet breakup in a measurement plane 15 mm from the nozzle tip across the three measurement positions. In this plane for all fuels, 60,000 droplets were detected. For the low temperature case, the averaged droplet sizes are very similar for n-hexane, n-heptane and the 3-component fuel, see Fig. 9. However, for n-decane, the averaged droplet size is approximately 5-7% smaller compared to the other fuels which is contrary to expectations following Lee and Reitz [23] who reported an increase of the droplet size proportional to the fuel viscosity. This is mainly due to aerodynamic breakup which is promoted by low viscosity and surface tension. Hence, the data presented above indicates that the aerodynamic jet and droplet breakup can not be the

main reason for the reduced droplet size of n-decane. This is caused by the dominance of the fuel viscosity on internal nozzle flow which controls primary spray breakup and the injected fuel mass. Under these partial load conditions, the small injected mass is 2.7% lower for n-decane, which is in agreement with the lower scattering intensity in the Mie images (see Figure 8) due to a reduced optical density of the spray. The viscosity dependent primary breakup (esp. the microscopic spray cone angle and macroscopic cyclic spray fluctuations) are discussed, e.g., in [24].

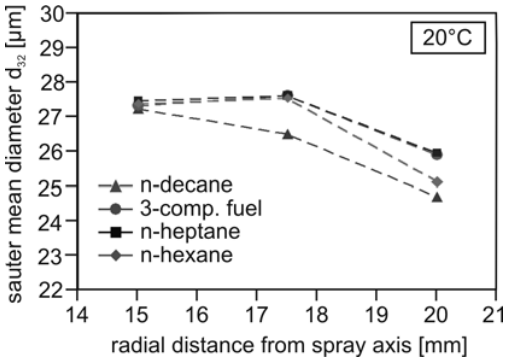

Figure 9: Time averaged drop sizes for the low temperature case across 3 locations in the measurement plane 15 mm from the nozzle tip

Numerical investigations with the calibrated spray model confirmed the reduced droplet size for larger fuel viscosity, but only after reducing the injected mass, see Fig. 10. It is to be noted that only secondary breakup effects were considered since the initial droplet size distribution modeling the primary atomization was kept constant. For a reduced injected mass, the Sauter mean diameter of the whole spray is approximately 1-2% smaller since frequency of collision occurrence lessens and aerodynamic drop breakup is enhanced for an optical thinner and more dilute spray. The differences in the experimentally determined droplet size are larger due to fuel dependence of turbulence and cavitation induced primary atomization that is not covered by the current model. However, the correct trend can be predicted by the simulations.

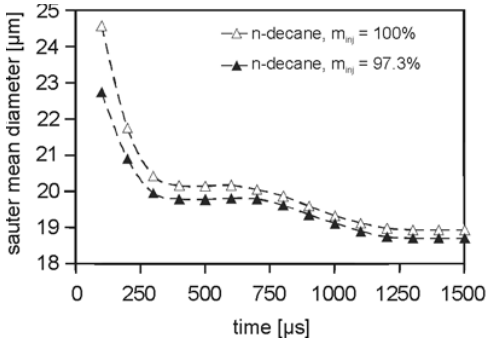

Figure 10: Temporal development of the calculated droplet sizes for the low temperature case, averaged for the whole spray, two injected masses, n-decane

Further investigations of the fuel-dependent nozzle flow and jet breakup can be found in [24].

SINGLE DROPLET EVAPORATION

Single droplet simulations applying the infinite diffusion model confirm the occurrence of separation of the fuel components in the droplet at the studied SG-DISI ambient conditions (1.5 MPa, 400°C), see Fig. 11. The results in the upper diagram indicate the characteristic heat-up period and the subsequent decline of the droplet surface for the single fuel components and the 3-component fuel. The delayed evaporation of the 3-component fuel becomes very distinct. This is due to the amount of the high boiling point fuel n-decane whose evaporation starts at 2 ms leading to an unsteady surface regression.

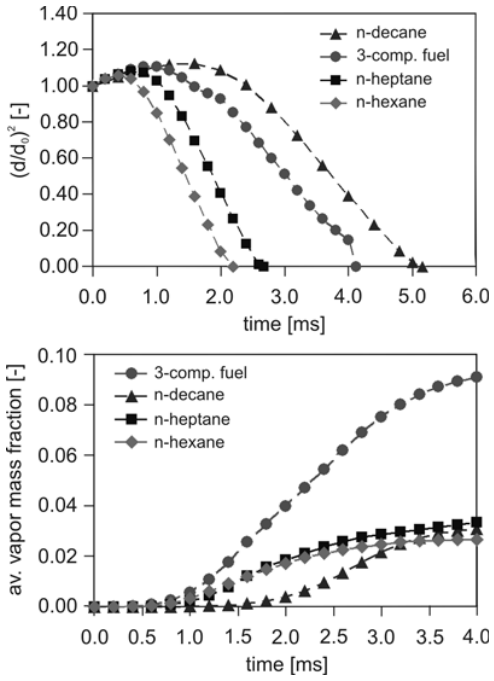

Figure 11: Results of the single droplet calculation, temporal reduction of the droplet size (top), averaged fuel vapor mass fraction in the surrounding gas phase of the of the 3-component fuel (bottom); p_C = 1.5 MPa, ϑ_C = 400°C, d_0 = 20 µm, ϑ_F = 70°C, u_{rel} = 0 m/s

In Fig. 11 (bottom diagram), the vapor mass fraction of the 3-component fuel is shown. The evaporation of n-hexane and n-heptane takes place almost simultaneously, whereas the increase of the vapor mass fraction of n-decane around the droplet is delayed. The vapor mass fraction is displayed as an average over the surrounding cells. These simulations were conducted for static droplets in quiescent air. However, also the relative velocity between the droplet and air in a spray would enhance the internal mixing in the fuel droplet and, therefore, the heat and mass transfer between the droplet and air as well as inside the droplet would be increased. Consequently, the whole spray process was calculated to study the sub-processes in detail.

SPRAY EVAPORATION

For the high temperature case, the evaporation effects dominate over the atomization processes that lead to distinct differences in droplet sizes. The average droplet size of n-decane is about 30% larger

compared to n-heptane, whereas the droplet diameter of n-hexane is approximately 25% smaller, see Fig. 12. The droplet diameter of the 3-component fuel is slightly larger than the droplet sizes of n-heptane. In the dilute outer region of the spray (18.5 mm), the averaged droplet sizes of n-heptane, the 3-component fuel and n-decane are very similar. There, the fuel-air interaction is increased, and the evaporation occurs very rapidly. Furthermore, the resulting evaporative cooling, which reduces the local evaporation rate, is less pronounced than in the centre of the spray and in the inner part (16.5 mm).

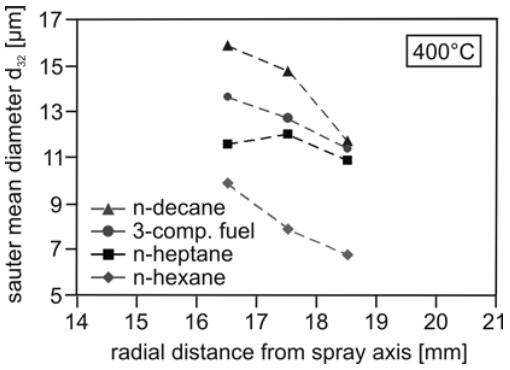

Figure 12: Averaged droplet sizes for high temperature conditions, measurement plane 15 mm from the nozzle tip

Finally, the calibrated spray model is applied to verify the fuel component distribution in the vapor phase of the spray and an occurrence of a possible stratification. In Fig. 13 the vapor distribution of the 3-component fuel is shown component-wise in an axial sectional plane (top) and along an orthogonal line at a distance of 15 mm from the nozzle tip (bottom). At first glance, the vapor distributions of the three components in the sectional planes appear very similar and only small differences in their propagation at the spray front are visible. This appears similar to the LIF-images of Hofmann et al. [9]. However, the quantification of the vapor content shows clear differences in their mass fractions. Especially, at the center line a local difference of 30% between n-heptane and n-decane is visible, which can be seen in the radial distribution (along a line in *x*-direction, see Fig. 13, bottom).

The spray-induced turbulence enhances the mixing of fuel components in the gas phase and, therefore, similar vapor clouds are visible. However, distinct local differences in the vapor mass fraction exist. In principle, according to the infinite diffusion model the components are uniformly distributed in the droplet and may evaporate simultaneously, but their evaporation rate and temporal behaviour is different due to their heat up period and boiling points. Therefore, a stratification of the fuel components in the vapor phase can be described with this model, see Fig. 13 (bottom). This is in agreement with the analytical estimation based on PDA measurements in [16]. The radial vapor mass fraction in the spray is displayed at 15 mm from the nozzle tip, which refers to ignition points in SG-DISI engines with late injection timing. The n-heptane shows the largest values of the local vapor mass fraction in accordance with its highest concentration in the mixture, and propagates further into the surrounding.

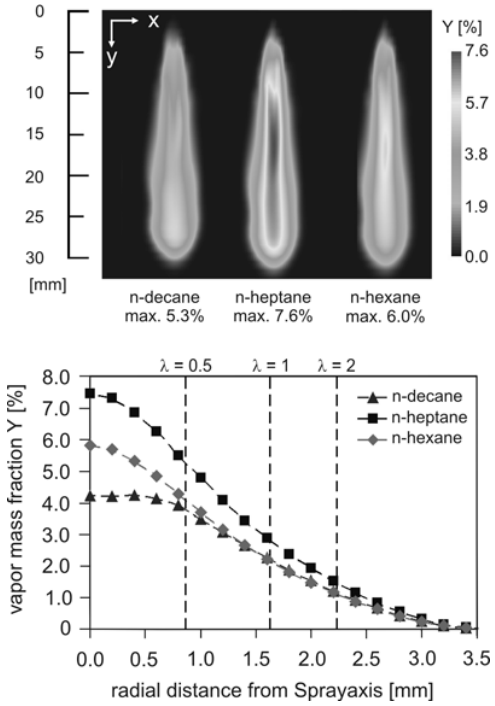

Figure 13: Planar vapor distribution of the 3-component fuel (top) and along a orthogonal line at 15 mm from the nozzle tip (bottom), p_C = 1.5 MPa, ϑ_C = 400°C, t = 1,000 µs

To asses the fuel composition effect on the inflammability, the ignitable range is discussed. Therefore, engine-relevant air ratios λ ($\lambda=1/\phi$, where ϕ is the equivalence ratio) are marked in the diagram. The ignitable range (at atmospheric conditions) refers to an air ratio of λ = 0.5…1.5; it has a width of approximately 1 mm and shows the complexity of the SG-DISI concept with charge stratification. Therein, the component with the largest amount in the fuel determines the ignitability. This effect can be more distinct for fuels with larger differences in fuel properties, e.g. when containing large fractions of ethanol. The maximum droplet lifetimes were compared to experimental data to validate the applied evaporation model. This model can cover the main effects of a relatively slow distillation-like evaporation process but shows a distinct heat-up period. The maximum droplet lifetimes were determined in two PDA-measurement planes at 10 and 15 mm from the nozzle tip. The values include all effects like droplet formation, breakup, turbulent dispersion, collision and evaporation. For n-hexane, the latest droplets in the spray were detected at 1.3 ms after SOI, the maximum droplet lifetime was determined for n-decane (1.9 ms), see Table 5. In comparison, the calculated maximum droplet lifetimes of the different fuels are given in Figure 14. As per definition, this lifetime refers to a time when the evaporated droplet mass exceeds 99%. This shows the good agreement between the model and the experimental results. The maximum droplet lifetime of n-decane is approximately 15% longer than in the experiment which is probably due to the widespread heat-up period in the infinite diffusion limit model.

Table 5: Maximum droplet lifetimes, experimental values extracted from [16]

	n-hexane	n-heptane	3-comp. f.	n-decane
Sim. [ms]	1.25	1.4	1.65	2.2
Exp. [ms]	1.3	1.5	1.6	1.9

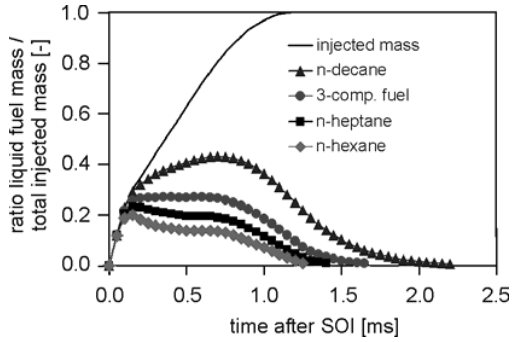

Figure 14: Trend of the injected liquid mass and remaining liquid fuel masses in the calculation domain. The maximum droplet lifetime can be estimated at the time point when 99% of fuel is evaporated.

In general, the evaporation time can be adjusted with different evaporation model approaches, e.g. with different formulations of the convective heat and mass transfer in the gas phase (see, e.g. [25]) or by the finite-diffusion model to delay the internal droplet mixing, which leads to a decreased heat-up phase.

CONCLUSION

An experimental and numerical work was conducted to study the fuel-dependent atomization and evaporation behavior under SG-DISI conditions with late injection timing. The sprays of three single and one 3-component fuels were analyzed with Mie scattering and phase Doppler anemometry in an injection chamber. A numerical model was set up based on these experimental data. The atomization was found to be dominated by the fuel viscosity; higher values resulted in a reduced injected mass and a more dilute spray. This leads to an enhanced droplet breakup and results in smaller droplets, which can be confirmed by the CFD-model after adjusting the fuel mass. The applied simple approach of multi-component evaporation based on the infinite-diffusion model predicts a fractionated evaporation of the fuel components. A stratification of the components in the vapor phase in the combustion chamber can be described for late injection timing conditions, which is in agreement with previously conducted analytical estimations based on PDA-measurements in [16]. A changed λ-distribution due to this stratification can be covered by this numerical approach. Therefore, a simple multi-component fuel should be preferably applied in simulations as well as experiments since a more realistic behaviour of the gasoline spray process results. Especially, for modern fuel mixtures with a high amount of biogenic or synthetic fuels, a distillation-like evaporation of the components and the altered ignition must be accounted. If the major fuel properties are comprised, this fuel behavior can be predicted by trend with the CFD-model. Additional variations of the fuel properties (and their combinations) are necessary to identify and describe their dominant effects on the respective spray sub-processes. Further, the analysis of fuel dependence of primary breakup is being investigated.

ACKNOWLEDGMENTS

The authors gratefully acknowledge the financial support of parts of this work of the Erlangen Graduate School in Advanced Optical Technologies (SAOT), which is funded by the German National Science Foundation (DFG) within the framework of the German Excellence Initiative. The authors thank the German Academic Exchange Service (DAAD) for funding the scholarship of Mr. Vivek Gupta within the WISE program.

DEFINITIONS, ACRONYMS, ABBREVIATIONS

ATDC	After TDC
BDC	Bottom Dead Center
BTDC	Before TDC
CA	Crank Angle
DISI	Direct Injection Spark Ignition
EOI	End of Injection
Exp	Experiment
IC	Internal Combustion
PDA	Phase Doppler Anemometry
SG	Spray Guided
SOI	Start of Injection
v. SOI	visible Start of Injection
SI	Spark Ignition
Sim	Simulation
TDC	Top Dead Center

d	diameter [m]
ϕ	equivalence ratio [-]
λ	air ratio [-]
p	pressure [bar] or [MPa]
r	radius [m]
t	time [s]
Y	vapor mass fraction [-] or [%]
ϑ	temperature [°C]
ω	frequency [Hz]

INDICES

bu	breakup
C	chamber
d	droplet
g	gas
F	fuel
L	liquid
rel	relative

REFERENCES

1. M.C. Lai, Y. Zheng, A. Matsumoto, J. Wang, X. Zhang, S. Moon, J. Gao, K. Fezzaa, L. Zigan, I. Schmitz, M. Wensing, A. Leipertz: Characterisation of Internal Flow and Spray of Multihole DI Gasoline Spray using X-Ray Imaging and CFD, SAE Technical Paper Series JSAE 20119225, SAE 2011-01-1881 (2011)
2. S.H. Park, H.K. Suh, C.S. Lee: Effect of Cavitating Flow on the Flow and Fuel Atomization Characteristics of Biodiesel and Diesel Fuels. Energy & Fuels, 22 , p. 605-613 (2008)
3. A. Sou, S. Hosokawa, A. Tomiyana: Effects of cavitation in a nozzle on liquid jet atomization. Int. J. Heat Mass Transfer, 50, p. 3575-3582 (2007)
4. G. Stiesch: Modeling Engine Spray and Combustion Processes. Springer-Verlag, Berlin (2004)
5. P.L. Kelly-Zion, J.P. Styron, C.-F. Lee, R.P. Lucht, J.E. Peters, R. A. White: Multicomponent liquid and vapour fuel measurements in the cylinder of a portinjected, spark ignition engine. Proceedings of the Combustion Institute, 27, 2, p. 2111–2117 (1998)
6. B. Williams, P. Ewart, R. Stone, H. Ma, H. Walmsley, R. Cracknell, R. Stevens, D. Richardson, J. Qiao, S. Wallace: Multi-Component Quantitative PLIF: Robust Engineering Measurements of Cyclic Variation in a Firing Spray-Guided Gasoline Direct Injection Engine. SAE Technical Paper Series 2008-01-1073 (2008)
7. D. Han, R.R. Steeper: An LIF equivalence ratio imaging technique for multicomponent fuels in an IC engine Proceedings of the Combustion Institute, 29, p. 727–734 (2002)
8. J. Egermann, A. Leipertz: Influence of Fuel Properties on Mixture Formation: An Experimental Analysis for High Pressure Swirl Injectors. SAE Technical Paper Series 2000-01-2863 (2000)
9. T. Hoffmann, P. Hottenbach, H.-J. Koss, C. Paul, G. Grünefeld: Investigation of Mixture Formation in Diesel Sprays under Quiescent Conditions using Raman, Mie and LIF Diagnostics. SAE Technical Paper 2008-01-0945 (2008)
10. L. Zigan, A. Flügel, I. Schmitz, M. Wensing, A. Leipertz: Structure of evaporating single- and multi-component fuel sprays for 2nd generation gasoline direct injection. Fuel, 90, p. 348–363 (2011)
11. L. Zigan, I. Schmitz, A. Flügel, M. Wensing, A. Leipertz: Influence of fuel properties on spray formation and evaporation measured on a piezoelectric injector for second-generation gasoline direct injection. Proceedings of Injection Systems for IC engines, I Mech E Paper C677/007/09, London, p. 193-202 (2009)
12. Fluidat on the net V1.18/5.70 - massflow and physical properties calculator. online available at: www.fluidat.com
13. J.D. Pandey, V. Vyas, P. Jain, G.P. Dubey, N. Tripathi, R. Dey: Speed of sound, viscosity and refractive index of multicomponent systems: theoretical predictions from the properties of pure components. Journal of Molecular Liquids, 81, p. 123-133 (1999)
14. V. Wagner, J. Goldlücke, O. Seelig, A. Leipertz: Potential von Mehrkomponentenkraftstoff für eine quantitative Gemischbildungsanalyse mit laserinduzierter Fluoreszenz. Engine Combustion Processes – Current Problems and Modern Techniques (VIth Congress), BEV-Heft 3.1, p. 251 - 261 (2003)
15. J.A. Dean: Lange's Handbook of Chemistry. McGraw-Hill, Inc. (1999)
16. L. Zigan, I. Schmitz, A. Flügel, T. Knorsch, M. Wensing, A. Leipertz: Effect of Fuel Properties on Spray Breakup and Evaporation Studied for a Multi-Hole Direct Injection Spark Ignition (DISI) Injector. Energy & Fuels, 24, p. 4341–4350 (2010)
17. F.X. Tanner: Liquid Jet Atomization and Droplet Breakup Modeling of Non-Evaporating Diesel Fuel Sprays. SAE Technical Paper Series 970050 (1997)
18. P.J. O'Rourke, A.A. Amsdan: The TAB Method for Numerical Calculation of Spray Droplet Breakup. SAE Technical Paper Series 872089 (1987)
19. P.J. O'Rourke, F.V. Bracco: Modeling Drop Interactions in Thick Sprays and a Comparison with Experiments. Proceedings of I Mech E, 9, p. 101-116 (1980)
20. N. Nordin: Complex Chemistry Modeling of Diesel Spray Combustion. PhD thesis, Chalmers University of Technology, Göteborg (2001)
21. W.A. Sirignano: Fluid Dynamics and Transport of Droplets and Sprays. Cambridge University Press, Cambridge, U.K. (1999)
22. D. Stegemann, G.P. Merker: Modeling the Evaporation of Multicomponent Diesel Fuel under Engine Conditions. ILASS-Europe 2005, 20th Annual Conference on Liquid Atomization and Spray Systems, Orléans (France) (2005)
23. K. Lee, R.D. Reitz: Investigation of spray characteristics from a low-pressure common rail injector for use in a homogeneous charge compression ignition engine. Measurement Science and Technology, 15, S. 509-519 (2004)
24. L. Zigan, I. Schmitz, M. Wensing, A. Leipertz: Effect of fuel properties on primary breakup and spray formation studied at a gasoline 3-hole nozzle. ILASS – Europe 2010, 23rd Annual Conference on Liquid Atomization and Spray Systems, Brno, Czech Republic (2010)
25. L. Zigan, M. Ammon, V. Gupta, I. Schmitz, M. Wensing, A. Leipertz: Analysis of Fuel Effects on Spray Atomization and Evaporation Studied at a Multihole DISI Injector for Late Injection Timing. Proceedings of the European Combustion Meeting, Cardiff (2011)

CONTACT

Lehrstuhl für Technische Thermodynamik, Universität Erlangen-Nürnberg, Am Weichselgarten 8, D-91058 Erlangen, Germany

Corresponding author:
Lars Zigan
Tel. +49-9131-8529770
E-Mail: lars.zigan@cbi.uni-erlangen.de
Homepage: www.ltt.uni-erlange